



HAL
open science

Analysis of three-dimensional physical quantities for system diagnosis

Gailene Shih-Lyn Phua, Pierre Granjon

► **To cite this version:**

Gailene Shih-Lyn Phua, Pierre Granjon. Analysis of three-dimensional physical quantities for system diagnosis. CM 2012 - 9th International Conference on Condition Monitoring and Machinery Failure Prevention Technologies, Jun 2012, Londres, United Kingdom. pp.n/a. hal-00690997

HAL Id: hal-00690997

<https://hal.science/hal-00690997>

Submitted on 25 Apr 2012

HAL is a multi-disciplinary open access archive for the deposit and dissemination of scientific research documents, whether they are published or not. The documents may come from teaching and research institutions in France or abroad, or from public or private research centers.

L'archive ouverte pluridisciplinaire **HAL**, est destinée au dépôt et à la diffusion de documents scientifiques de niveau recherche, publiés ou non, émanant des établissements d'enseignement et de recherche français ou étrangers, des laboratoires publics ou privés.

Analysis of three-dimensional physical quantities for system diagnosis

Journal:	<i>CM 2012 and MFPT 2012</i>
Manuscript ID:	CM-MFPT-0043-2012.R1
Topic:	Other (specify below)
Date Submitted by the Author:	n/a
Complete List of Authors:	Phua, Gailene; Gipsa-lab, DIS Granjon, Pierre; Gipsa-lab, DIS
Keywords:	Condition monitoring, Signal processing, Signal analysis

Topic:

Condition monitoring (CM) methods and technologies

Title:

Analysis of 3D physical quantities for system diagnosis

Authors:

Phua, Gailene; Gipsa-lab

Granjon, Pierre; Gipsa-lab

Abstract:

Most methods for system diagnosis are based on analysis of three-dimensional physical quantities. For example, electrical system monitoring is based on three-phase electrical measurements and 3D vibration analysis involves studying three-dimensional mechanical measurements. In three-dimensional space, such quantities follow a trajectory whose geometric characteristics are representative of the state of the monitored system. Usual techniques for diagnosis analyze such quantities component by component, without taking into account their three-dimensional nature or the geometric characteristics of their trajectory. A significant part of the information that may be useful for diagnosis is thus ignored. The main objective of this work is to estimate the geometric characteristics and trajectories of three-dimensional quantities using basic differential geometry concepts with the aim of developing tools for processing and analyzing 3D data. Such tools provide additional information for system diagnosis with respect to conventional methods and therefore increase their performance in terms of fault detection and localization. Simulated and experimental data concerning electrical power systems will be used to demonstrate the usefulness of this approach.

Analysis of three-dimensional physical quantities for system diagnosis

Gailene S L Phua and Pierre Granjon

Gipsa-lab

11, rue des Mathématiques,

Grenoble Campus,

38402 Saint-Martin-d'Hères,

France.

Telephone: +33476574354

E-mail: gailene-shih-lyn.phua@gipsa-lab.grenoble-inp.fr

Abstract

Most methods for system diagnosis are based on the analysis of three-dimensional or three-component physical quantities or signals. For example, electrical system monitoring is based on three-phase electrical measurements and three-dimensional vibration analysis involves studying three-directional mechanical measurements. In three-dimensional space, such physical quantities follow a trajectory whose geometric properties are representative of the state of the monitored system. Usual techniques for diagnosis analyze these signals component by component, without taking into account their three-dimensional nature or the geometric properties of their trajectory. A significant part of the information that may be useful for diagnosis is thus ignored. The main objective of this work is to estimate the geometric properties of three-dimensional physical quantities using basic differential geometry concepts with the aim of developing tools for processing and analyzing three-dimensional signals. Such tools provide additional information for system diagnosis with respect to conventional methods and therefore increase their performance in terms of fault detection and localization. Simulated and experimental data concerning electrical power systems are used to demonstrate the usefulness of this approach.

1. Introduction

Most condition monitoring techniques rely on the characterization of inherently three-component physical quantities. A classic example is the monitoring of three-phase electrical systems, based on three-phase electrical measurements or three-dimensional magnetic stray field measurements. Another common example is the monitoring of mechanical systems, based on triaxial or three-dimensional vibration measurements. When represented in a three-dimensional space (or Euclidean space), such quantities follow a curve whose geometric characteristics contain information concerning the state of the monitored system. However, conventional condition monitoring methods most often analyze such quantities as three separate components, without taking into account the three-dimensional geometric characteristics of their trajectory. As a consequence, a significant part of the diagnostic information is ignored.

This work aims to fill this gap by presenting a method to estimate geometric characteristics or geometric indicators of three-component signals. This method relies on basic differential geometry concepts such as the Frenet frame, curvature, and torsion,

and leads to local geometric descriptors of the three-dimensional curves followed by three-component signals. There are three main parts in this paper. The basic differential geometry tools used in this study are presented in Section 2, along with useful local geometric descriptors of three-dimensional curves. In Section 3, an algorithm is proposed to estimate such descriptors from three-component measurements. Finally, an application example concerning the monitoring of three-phase voltage dips in power networks is presented in section 4.

2. Definition of three-dimensional geometric indicators

In this section, the measured components $r_1(\mathbf{t})$, $r_2(\mathbf{t})$ and $r_3(\mathbf{t})$ of a three-component signal are considered as the Cartesian coordinates of a particle moving with respect to time \mathbf{t} along a trajectory in the Euclidean space. These three components form a vector-valued function $\mathbf{r}(\mathbf{t})$ of class \mathcal{C}^p (i.e. p times continuously differentiable), and which depends on the parameter \mathbf{t} . $\mathbf{r}(\mathbf{t})$, also known as the position vector, is then defined by:

$$\mathbf{r}(\mathbf{t}) = \begin{bmatrix} r_1(\mathbf{t}) \\ r_2(\mathbf{t}) \\ r_3(\mathbf{t}) \end{bmatrix} \quad (1)$$

This function can be viewed as a parametric three-dimensional \mathcal{C}^p ($p \geq 3$) curve with parameter \mathbf{t} , and with interesting geometric properties we want to study. In the rest of this section, classical differential geometry quantities which allow efficient analysis of the geometric properties of 3D curves are presented. See for example the classical books on differential geometry [1]-[4] to obtain a more formal description of these quantities.

2.1 Frenet frame

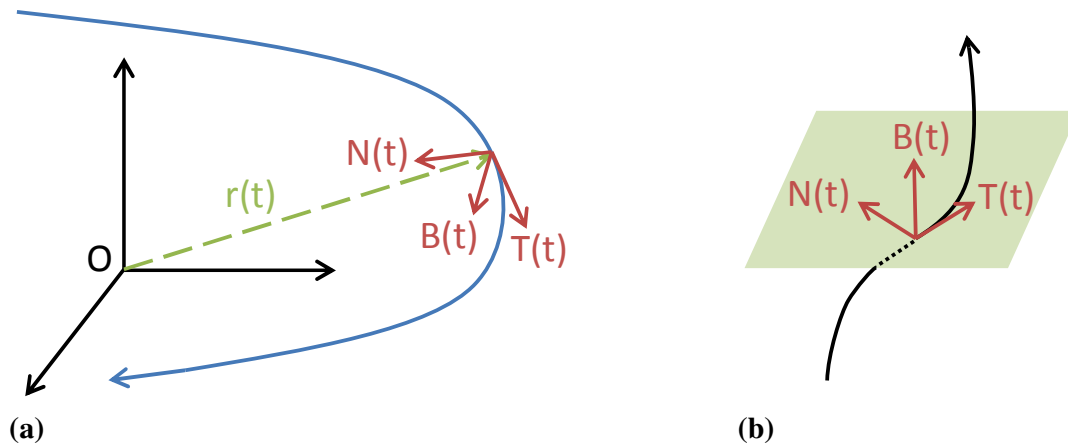


Figure 1. The Frenet frame. (a) Tangent, normal and binormal vectors $\mathbf{T}(\mathbf{t})$, $\mathbf{N}(\mathbf{t})$ and $\mathbf{B}(\mathbf{t})$ of a curve at point $\mathbf{r}(\mathbf{t})$. (b) Osculating plane of a curve containing the tangent and normal vectors.

The Frenet frame is a moving reference frame on three orthogonal vectors used to locally describe a curve at each point. It is the main tool in differential geometric

processing and analysis of curves, since it is far easier and more natural to describe local geometric properties in terms of a local reference system than using a global one like the Euclidean coordinates.

The Frenet frame can be directly defined from the position vector $\mathbf{r}(\mathbf{t})$ as follows:

$$\begin{aligned} T(\mathbf{t}) &= \frac{\mathbf{r}'(\mathbf{t})}{\|\mathbf{r}'(\mathbf{t})\|} \\ N(\mathbf{t}) &= \frac{T'(\mathbf{t})}{\|T'(\mathbf{t})\|} = \frac{\mathbf{r}'(\mathbf{t}) \times (\mathbf{r}''(\mathbf{t}) \times \mathbf{r}'(\mathbf{t}))}{\|\mathbf{r}'(\mathbf{t})\| \|\mathbf{r}''(\mathbf{t}) \times \mathbf{r}'(\mathbf{t})\|} \\ B(\mathbf{t}) &= T(\mathbf{t}) \times N(\mathbf{t}) = \frac{\mathbf{r}'(\mathbf{t}) \times \mathbf{r}''(\mathbf{t})}{\|\mathbf{r}'(\mathbf{t}) \times \mathbf{r}''(\mathbf{t})\|} \end{aligned} \quad (2)$$

where “ \times ” denotes the vector product or cross product and “ $\|\cdot\|$ ” denotes the vector norm. $\mathbf{r}'(\mathbf{t})$ is the first derivative of \mathbf{r} at time \mathbf{t} or $\frac{d\mathbf{r}}{dt}$ and is also called the velocity vector. Similarly, $\mathbf{r}''(\mathbf{t})$ is the second derivative of \mathbf{r} at time \mathbf{t} or $\frac{d^2\mathbf{r}}{dt^2}$ and is also referred to as the acceleration vector.

As can be seen in Figure 1(a), the three unit orthogonal vectors defining the Frenet frame are:

- $T(\mathbf{t})$ the tangent vector,
- $N(\mathbf{t})$ the normal vector, and
- $B(\mathbf{t})$ the binormal vector.

The tangent vector $T(\mathbf{t})$ can be seen as the direction that a point is following as it moves along a curve. The normal vector $N(\mathbf{t})$ represents the direction of change in the tangent vector as it changes with respect to time. The binormal vector $B(\mathbf{t})$ is used to characterize the orientation of the plane which contains the curve. This plane is also known as the osculating plane, and an example is represented in Figure 1(b). When the binormal vector of a curve changes, it means that at the same time the osculating plane changes its orientation.

2.2 Frenet-Serret formulas

The Frenet-Serret formulas describe the kinematic properties of $\mathbf{r}(\mathbf{t})$ which moves along a curve in three-dimensional Euclidean space, and leads to the geometric properties of the curve itself. More specifically, the formula describes the derivatives of the unit tangent, normal, and binormal vectors in terms of each other as follows:

$$\frac{d}{dt} \begin{bmatrix} T(\mathbf{t}) \\ N(\mathbf{t}) \\ B(\mathbf{t}) \end{bmatrix} = \|\mathbf{r}'(\mathbf{t})\| \begin{bmatrix} 0 & \kappa(\mathbf{t}) & 0 \\ -\kappa(\mathbf{t}) & 0 & \tau(\mathbf{t}) \\ 0 & -\tau(\mathbf{t}) & 0 \end{bmatrix} \begin{bmatrix} T(\mathbf{t}) \\ N(\mathbf{t}) \\ B(\mathbf{t}) \end{bmatrix} \quad (3)$$

where $\kappa(\mathbf{t})$ is the curvature and $\tau(\mathbf{t})$ the torsion of the curve at the point $\mathbf{r}(\mathbf{t})$. This equation clearly shows that the quantities $\mathbf{r}'(\mathbf{t})$, $\kappa(\mathbf{t})$ and $\tau(\mathbf{t})$ are sufficient to completely describe the kinematic properties of the trajectory followed by $\mathbf{r}(\mathbf{t})$, and that these three quantities contain the whole geometric information necessary to describe the corresponding curve.

2.3 Curvature and torsion

There are several ways to express the curvature and the torsion of a curve. The two following equations give these expressions directly as a function of $\mathbf{r}(\mathbf{t})$:

$$\begin{aligned}\kappa(\mathbf{t}) &= \frac{\|\mathbf{r}'(\mathbf{t}) \times \mathbf{r}''(\mathbf{t})\|}{\|\mathbf{r}'(\mathbf{t})\|^3} \\ \tau(\mathbf{t}) &= \frac{(\mathbf{r}'(\mathbf{t}) \times \mathbf{r}''(\mathbf{t})) \cdot \mathbf{r}'''(\mathbf{t})}{\|\mathbf{r}'(\mathbf{t}) \times \mathbf{r}''(\mathbf{t})\|^2}\end{aligned}\quad (4)$$

where “ \cdot ” denotes the dot product.

Every point of a circle has a curvature κ which is constant and equal to the reciprocal of its radius R . For example, smaller circles bend more sharply, and thus have greater curvature. The torsion of a curve is the rate of change of the orientation of the osculating plane. It measures how sharply a curve is twisting. When a curve stays in the same plane, the osculating plane is then constant and the torsion is zero. The torsion is nonzero when the curve twists into a different osculating plane, i.e. with a different orientation and thus a different binormal vector.

2.4 Preliminary assumptions on signals

In order to obtain simple three-dimensional trajectories, several assumptions are made about the measured signals:

- Each component $r_1(\mathbf{t})$, $r_2(\mathbf{t})$ and $r_3(\mathbf{t})$ is composed of a sine wave with the same constant frequency f_0 .
- The amplitude and phase of each sinusoidal component are either constant or slowly varying.

Under these assumptions, it can be shown that the trajectory followed by the position vector is locally plane, and that the corresponding curve can only be in the shape of a circle or an ellipse. Moreover, the geometric properties of this curve are directly related to the values of the amplitude and phase of each sinusoid. Finally, each of the continuous-time signals $r_1(\mathbf{t})$, $r_2(\mathbf{t})$ and $r_3(\mathbf{t})$ are sampled with sampling rate f_s which satisfies the sampling theorem and verifies $f_s \gg 2f_0$. We then obtain $\mathbf{r}[k]$, the discrete-time version of the position vector given in Eq. (1).

In this section, Eqs. (2) and (4) show that the geometric properties of a three-dimensional curve such as the tangent, normal and binormal vectors as well as the

curvature and torsion at any point of the curve can be easily computed with the first three derivatives of $\mathbf{r}(\mathbf{t})$. In the next section, we present the algorithm relying on these two equations and we show that it is possible to estimate these geometric indicators from the discrete position vector $\mathbf{r}[k]$.

3. Estimation of three-dimensional geometric indicators

Eqs. (2) and (4) give us the geometric properties that are to be estimated. The algorithm used to estimate these geometric indicators is explained in this section. It is made up of three main steps as shown in the block diagram in Figure 2. The three-component signal is first lowpass filtered to remove high-frequency noise and to select the component of frequency f_0 . It is then differentiated three times with a simple differentiation method and finally, the computation of the various geometric properties of the corresponding curve is carried out thanks to Eqs. (2) and (4). Each of these steps is explained in the following.

3.1 Lowpass filtering

The three-component signal must be filtered of any high-frequency components before differentiation because this last operation significantly amplifies such components possibly present in the signal^[5]. The signal is also filtered to limit its frequency content to f_0 and to select only the corresponding sine wave. In the proposed algorithm, this filter is a simple lowpass linear-phase finite impulse response filter designed using the classical Kaiser window method^{[6][7]}.

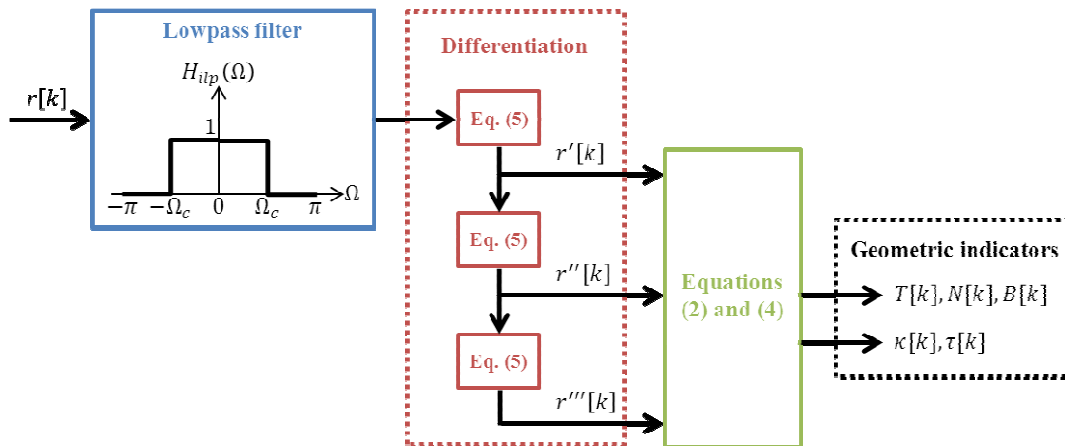


Figure 2. The proposed algorithm to estimate the geometric properties of three-component signals.

3.2 Differentiation method

Eqs. (2) and (4) show that differentiation is needed to estimate the geometric properties of curves. There are many different methods of differentiation^[5] but a simple and intuitive method is chosen for this study. The derivative of a point of a curve is equal to the slope of the curve at this particular point, which corresponds mathematically to:

$$r'[k] = \frac{r[k+1] - r[k-1]}{2T_s} \quad (5)$$

This approximation is sufficient to compute the derivative of the signal because the frequency f_b of the sinusoidal component is very low compared to the sampling frequency f_s . In the proposed algorithm, the signal is differentiated three times using Eq. (5) to obtain $r'[k]$, $r''[k]$ and $r'''[k]$ before moving on to the next step which is to compute the desired geometric indicators.

3.3 Computation of geometric indicators

When the derivatives of the position vector $r'[k]$, $r''[k]$ and $r'''[k]$ have been obtained, the geometric properties of the curve $\Gamma[k]$, $N[k]$, $B[k]$, $\kappa[k]$ and $\tau[k]$ can finally be computed using Eqs. (2) and (4) with a combination of basic mathematical tools such as the dot product, the cross product and the modulus.

The previous three steps form the proposed algorithm to estimate the geometric properties of three-component signals. They rely on simple signal processing tasks such as linear and time-invariant filters, differentiations and products and can therefore be easily implemented in real-time if necessary.

However, some precautions must be taken to use this algorithm. The discrete filter described in Section 3.1 must have sufficient performance to efficiently cancel out the high-frequency content of the signals before differentiation. If necessary, this filtering operation can be improved by using a better filter design method, or by using an infinite impulse response filter. Moreover, the derivative estimate given in Eq. (5) is only valid if the frequency content of the signals is very low with respect to the sampling frequency f_s . If this is not the case, more accurate estimation of derivatives should be used such as in [5].

The next section gives an example of application of the previous algorithm on simulated and three-phase voltage signals.

4. Application: Analysis of three-phase voltage dips

As an example, the previous method is applied to the study of voltage dips in three-phase power networks. These phenomena are the most common type of power-quality disturbances, and lead to important economic losses and distorted quality of industrial products. Thus, voltage dips monitoring has become an essential requirement for power quality monitoring^[8], and several methods have been developed to accurately detect and characterize such disturbances. However, most of these techniques consider three-phase measurements as three separate one-dimensional quantities, and process each phase voltage independently of each other^{[9][10]}. In [11], a first step is taken since the three-phase quantities are considered two-dimensional after a Clarke transform, and are processed as complex-valued signals. In this paper, we propose to apply the method

described in the previous sections in order to consider the three-phase voltages as a single three-dimensional quantity. The objective is not to obtain better results than previously proposed methods, but to adopt a different and complementary point of view by considering three-phase quantities as a whole.

The first three-phase voltages used in this section are the simulated data represented in Figure 3, and consist of a sine wave with fundamental frequency $f_0 = 50$ Hz sampled at sampling rate $f_s = 20$ kHz. It is clear from this figure that this three-phase voltage system undergoes a voltage dip on the blue voltage between $t = 0.05$ s and $t = 0.15$ s.

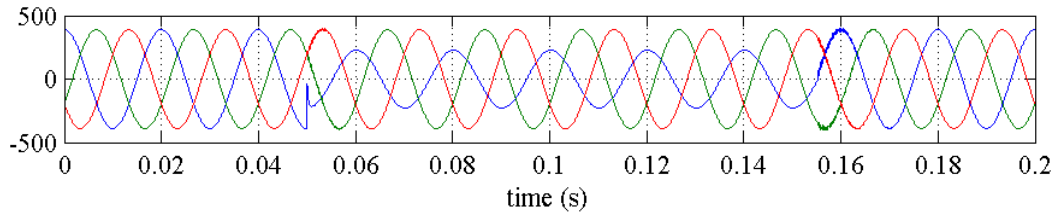


Figure 3. Simulated three-phase voltage signal.

The corresponding position vector $r[k]$ is constructed with the three previous voltages as described by Eq. (1). $r[k]$ is then represented as a moving point in an Euclidean space, and the corresponding curve is shown in Figure 4 its low-pass filtered version in Figure 5. This figure shows that $r[k]$ mainly rotates around the frame origin with frequency $f_0 = 50$ Hz. It can also be noticed that the three-dimensional trajectory followed by the position vector changes during the voltage dip. This remark justifies the use of the proposed method to analyze the geometric changes in this trajectory, and to eventually detect and/or characterize this voltage dip.

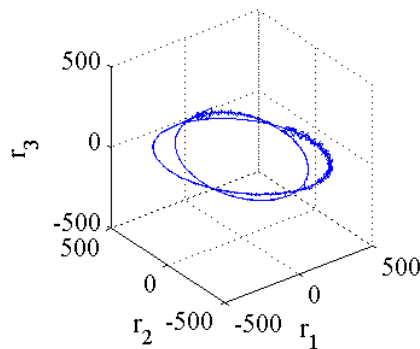


Figure 4. Three-component position vector in three-dimensional space.

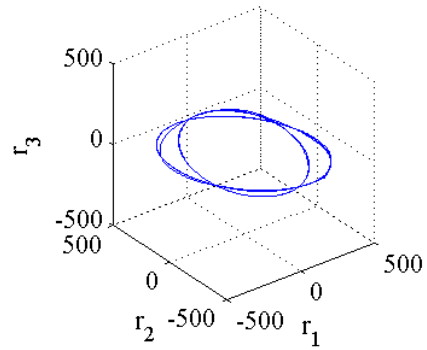


Figure 5. Three-component position vector in three-dimensional space after lowpass filtering.

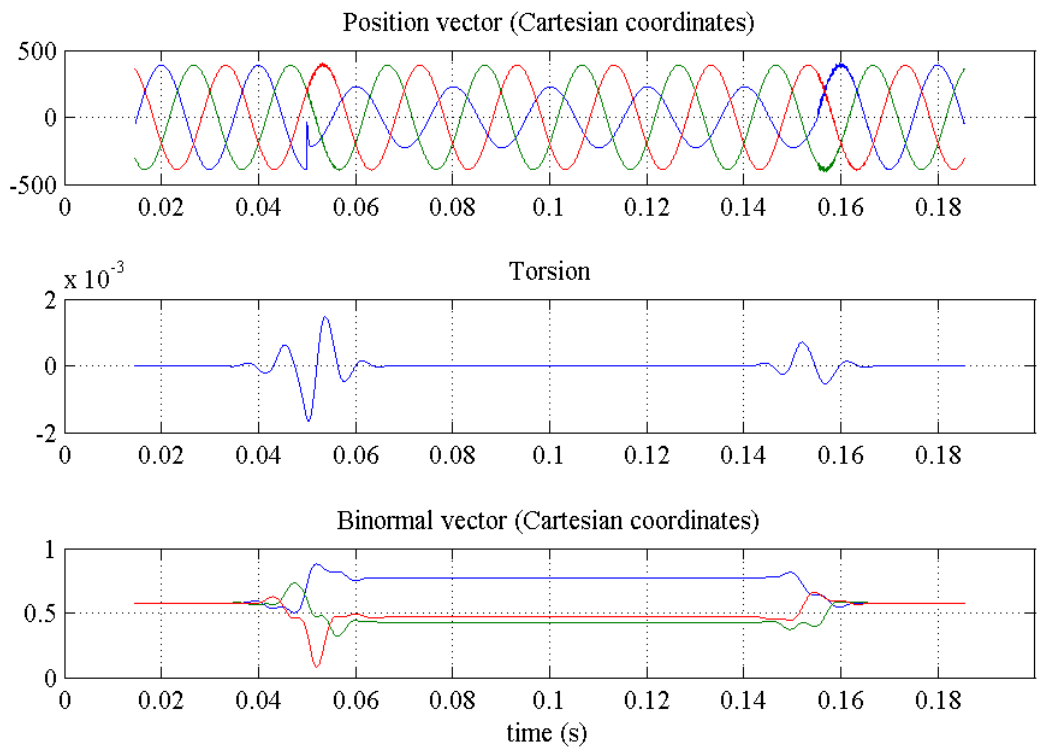


Figure 6. Simulated three-phase voltage signal, torsion and binormal vector.

The torsion corresponding to this curve is estimated thanks to the algorithm presented in the previous section, and represented in Figure 6 along with the three voltages. It can be noted that this torsion has large values only at the beginning and at the end of the voltage sag. Apart from these special moments, this quantity remains small and close to zero. Geometrically, this means that the three-dimensional curve followed by the point $r[k]$ belongs to a fixed plane, except at these precise moments during which the

osculating plane changes significantly. We also notice that the osculating plane containing the trajectory during and outside the voltage dip is not the same. This is highlighted by changes in the binormal vector, which is orthogonal to this plane. The Cartesian coordinates of this vector are also plotted in Figure 6, and they clearly take different values during and outside the dip.

The curvature is also estimated by this algorithm, and is represented in Figure 7. This geometric quantity leads to different information, related to the shape of the trajectory followed by $r[k]$. Outside the dip, the curvature remains constant and the trajectory is then circular. During the dip, the curvature varies with frequency $2f_0 = 100$ Hz, i.e. twice per revolution. If this quantity is compared to the magnitude of the position vector $\|r[k]\|$ also represented in Figure 7, it is clear that when the point $r[k]$ is close to the frame origin, the curvature is small and vice versa. This corresponds to a trajectory with an ellipse shape. Finally, the time evolution of the curvature shows that the point $r[k]$ changes from a circular trajectory outside the dip to an ellipse-shaped one during the dip.

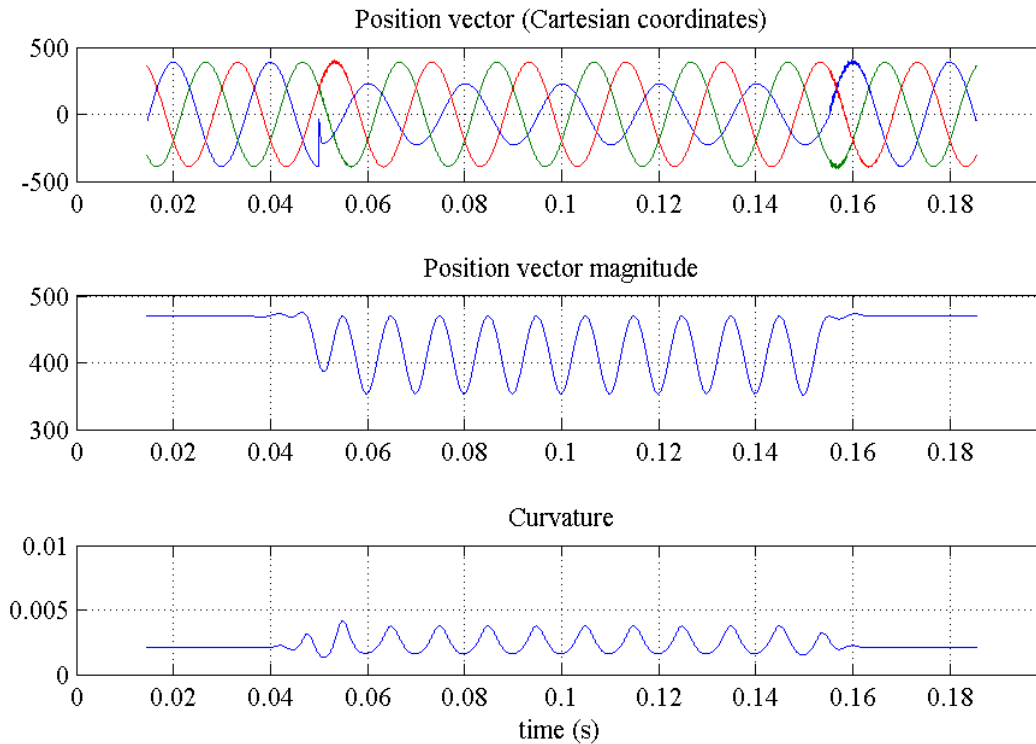


Figure 7. Simulated three-phase voltage signal, magnitude of position vector and curvature.

The results obtained through simulated data show that geometric quantities such as curvature and torsion lead to important geometric information concerning the three-dimensional trajectory followed by $r[k]$, and similarly to information about the state of the corresponding three-phase system.

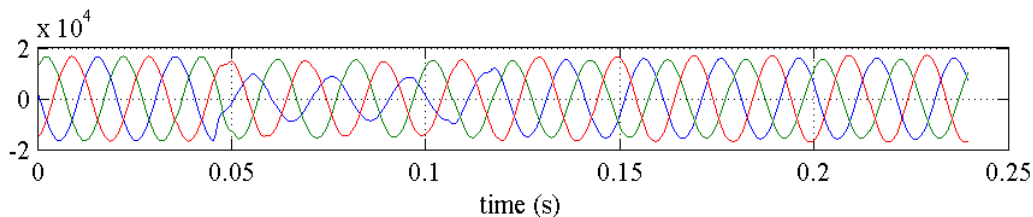


Figure 8. Experimental three-phase voltage signal.

The same method has also been applied to experimental three-phase voltages sampled at $f_s = 3200$ Hz. These data are represented in Figure 8, and clearly undergo a voltage dip between $t = 0.05$ s and $t = 0.12$ s, the dip being more important for the blue voltage. The corresponding three-dimensional trajectory is shown in Figure 9, with estimated torsion and curvature in Figure 10 and Figure 11 respectively. These experimental results are very similar to the previous ones obtained with simulated data. The main difference is visible in Figure 11 where it can be noticed that the magnitude of the position vector and the curvature keep oscillating after $t = 0.12$ s. This shows that the three-phase system still undergoes a small dip even after this moment.

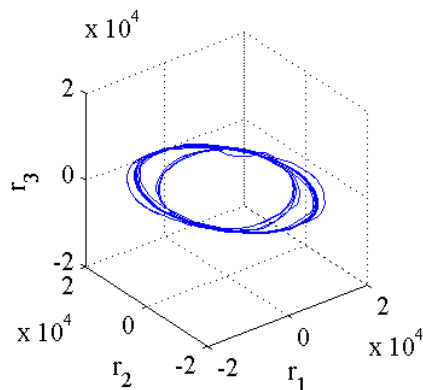


Figure 9. Three-component position vector in three-dimensional space.

From a practical point of view, the previous geometric indicators can be used to study and analyze voltage dips encountered in three-phase systems. For example, the modulus of the torsion can be used to detect the occurrence of such perturbations since it has important values at the beginning and at the end of dips. The detected dips can then be characterized thanks to the osculating plane given by the binormal vector coordinates, along with the curvature leading to information about the shape of the trajectory during the dips. However, this particular application is not finalized in this paper as this is not the main purpose of this work.

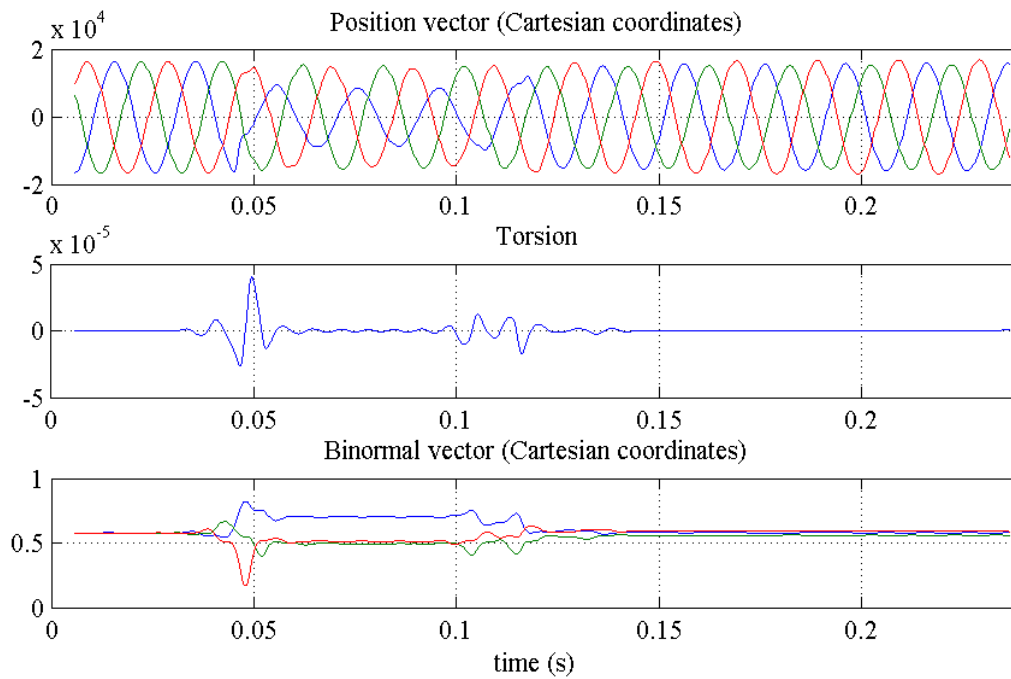


Figure 10. Experimental three-phase voltage signal, torsion and binormal vector.

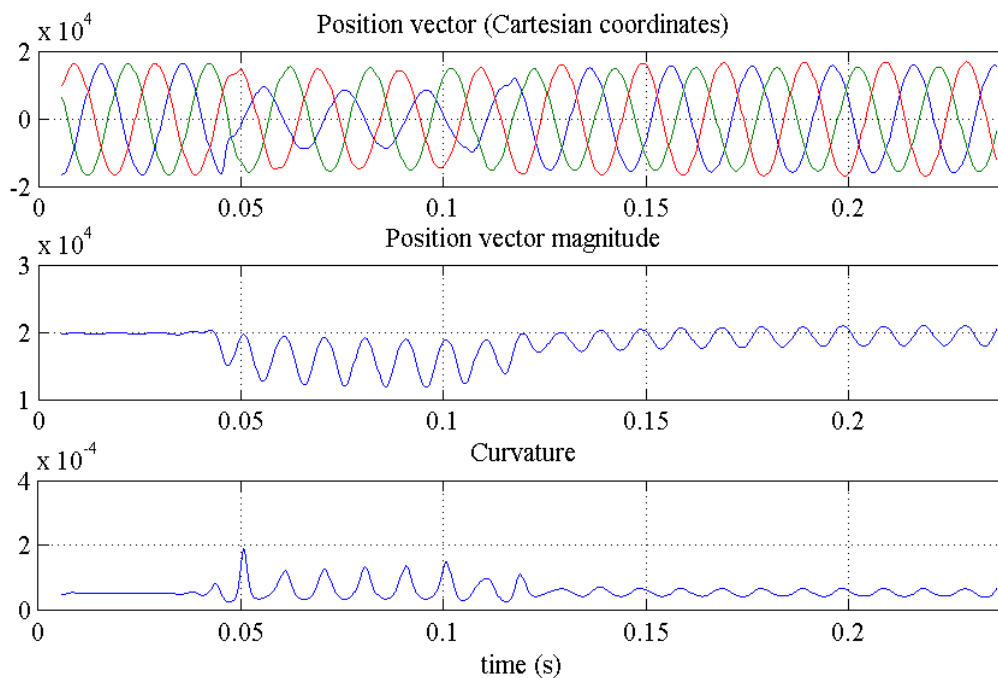


Figure 11. Experimental three-phase voltage signal, magnitude of position vector and curvature.

5. Conclusion

This paper presents a method dedicated to the monitoring of systems and based on the estimation and the analysis of geometric characteristics of three-component signals. It relies on classical differential geometry tools such as the Frenet frame and the curvature and torsion of three-dimensional curves. A simple and efficient algorithm realizing the estimation of these geometric indicators is also proposed and its application to simulated and experimental data leads to encouraging results. We can conclude from these results that the proposed method is useful as it gives different and complementary information to existing condition monitoring methods.

Of course some aspects of future work need to be addressed. For example, this method has to be extended to more complex deterministic signals (signals of arbitrary frequency f_0 or containing more than only one sinusoidal component), or even to random signals. These tools could also be applied to other types of three-component data such as triaxial vibrations, where the geometric characteristics are directly connected to those of three-dimensional movements in such systems and thus have clear physical significations.

References

1. M P do Carmo, 'Differential Geometry of Curves and Surfaces', Prentice-Hall, Englewood Cliffs, NJ, 1976.
2. E Kreyszig, 'Differential Geometry', Dover Publications, New-York, 1991.
3. M Spivak, 'A Comprehensive Introduction to Differential Geometry, Vol. 2', Publish or Perish, Berkeley, CA, 1990.
4. D J Struik, 'Lectures on Classical Differential Geometry', Addison-Wesley, Reading, Mass., 1961.
5. C C Tseng and S L Lee, 'Linear phase FIR differentiator design based on maximum signal-to-noise ratio criterion', Signal Processing, Vol 86, Issue 2, pp 388-398, February 2006.
6. J G Proakis and D G Manolakis, 'Digital Signal Processing: Principles, Algorithms, and Applications (Fourth Edition)', Pearson Education, NJ, 2007.
7. M Mandal and A Asif, 'Continuous and Discrete Time Signals and Systems', Cambridge University Press, UK, 2007.
8. M H Bollen, 'Understanding power quality problems: voltage sags and interruptions', Wiley-IEEE Press, New York, 1999.
9. M H Bollen and L D Zhang, 'Different methods for classification of three-phase unbalanced voltage dips due to faults', Elect. Power Syst. Res., Vol 66, No 1, pp 59-69, July 2003.
10. M H Bollen and I Y Gu, 'Signal processing of power quality disturbances', Wiley-IEEE Press, 2006.
11. V Ignatova, P Granjon and S Bacha, 'Space vector method for voltage dips and swells analysis', IEEE Trans. on Power Delivery, Vol 24, Issue 4, pp 2054-2061, October 2009.